JCTC Journal of Chemical Theory and Computation
Letter
pubs.acs.org/JCTC

Microstructure-Dependent Gas Adsorption: Accurate Predictions of Methane Uptake in Nanoporous Carbons

Yungok Ihm,[†] Valentino R. Cooper,*[,‡] Nidia C. Gallego,[‡] Cristian I. Contescu,[‡] and James R. Morris*[,‡,†]

[†]Department of Materials Science and Engineering, University of Tennessee, Knoxville, Tennessee 37996, United States
[‡]Materials Science and Technology Division, Oak Ridge National Laboratory, Oak Ridge, Tennessee 37831-6069, United States

Supporting Information

ABSTRACT: We present a framework for rapidly predicting gas adsorption properties based on van der Waals density functional calculations and thermodynamic modeling. Utilizing this model and experimentally determined pore size distributions, we are able to accurately predict uptakes in five activated carbon materials without empirical potentials or lengthy simulations. Our results demonstrate that materials with smaller pores and higher heats of adsorption can still have poor adsorption characteristics due to relatively low densities of highly adsorbent pores.

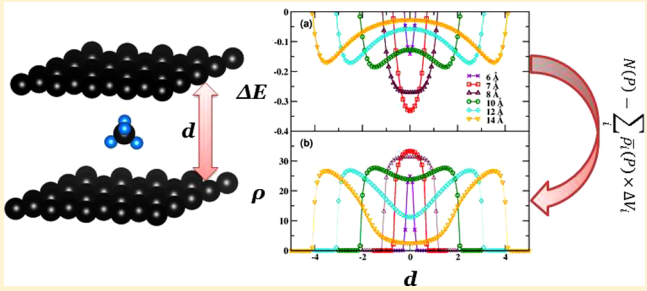

A key grand challenge in materials engineering is to select, design, and tune materials for specific capabilities. However, this is often difficult due in part to the important role of microstructure in determining properties. Adsorption properties correlate with pore volume, effective surface area, and pore size distribution,[1] but this does not provide sufficient predictive capability. More accurate predictions demand calculations of microstructure-dependent adsorbent−adsorbate interactions and modeling of thermodynamic equilibria,[2,3] with minimal experimental input. In particular, pore size and structure can modify adsorption properties, but only recently has this been quantified.[4]

Traditional approaches to modeling adsorption include the development of empirical adsorbent−adsorbate (and adsorbate−adsorbate) interactions[2,5,6] based primarily on fitting to experiment and then using Grand Canonical Monte Carlo (GCMC) simulations or a classical density functional theory (DFT) to describe equilibrium uptake.[7−12] A recent report proposes a complex hybrid method that involves quantum chemistry calculations combined with dispersion-corrected DFT calculations to obtain adsorption energy and a multisite Langmuir model using an adsorption equilibrium constant for individual adsorption sites to calculate adsorption isotherms.[13] While these methods have successfully described gas adsorption in carbon slit pores,[7−9] zeolites,[6,10,11] and metal−organic framework materials (MOFs),[12−14] one would ideally like to be able to screen materials using a methodology with minimal complexity and without the use of empirical potentials and/or lengthy simulations.

The purpose of this paper is to demonstrate this possibility using only minimal microstructural information with a specific example of methane storage on nanoporous carbon materials. Our method combines (1) an accurate description of adsorbent−adsorbate interactions using density functional theory incorporating long-range interactions (vdW-DF^{C09x})[15,16] and (2) an extremely fast thermodynamic model, described below, providing accuracy comparable to the GCMC method.[17,18] The approach provides a reliable and efficient method for rapidly screening the capabilities of any adsorbent materials for gas adsorption. In this paper, we successfully predict the methane uptake for five different activated carbons (ACs) comprised of highly complex pores with a range of pore sizes, resulting in very different uptake characteristics.

The primary assumption is that the pores of the activated carbons may be modeled as "slit pores" with graphene sheets separated by ≥5 Å. This is a reasonable approximation, as recent TEM and diffraction results show the presence of short-range graphitic order in these materials.[19−21] The potential energy surface (PES) for the CH_4−graphene sheet interaction was calculated using vdW-DF^{C09x}[15,16,22] as implemented in Quantum Espresso.[23] Recently, we demonstrated that this density functional gives an accurate description of H_2 adsorption on coronene, comparable to quantum chemistry calculations,[24] and can change predictions for optimal pore size for hydrogen storage in carbon slit pores.[18] The energy of methane in the slit pore geometry is calculated by summing the interactions between methane and graphene sheets separated by a distance corresponding to the pore size.

The CH_4−slit pore interaction energies are directly used to estimate the methane storage capacity of slit pores using a thermodynamic continuum model for gas adsorption.[18] Our thermodynamic model calculates the local pressure P_i of the adsorbed gas using

$$P_i = (\varphi_{ext}/\varphi_i) \times P_{ext} \times \exp(-E_i/k_B T)$$

Received: October 7, 2013
Published: November 27, 2013

dx.doi.org/10.1021/ct400875n | J. Chem. Theory Comput. 2014, 10, 1−4

where E_i and ϕ_i are the binding energy and fugacity coefficient of the adsorbed gas at the site i, respectively, and P_{ext} and ϕ_{ext} are the pressure and the fugacity coefficient of the external gas, respectively. The fugacity coefficients are calculated from

$$\ln \varphi = \int_0^p \left(\frac{V}{RT} - \frac{1}{p} \right) dp$$

using the $P-V$ data obtained from the equation of state of Setzmann and Wagner.[25] The local adsorption density is then calculated from P_i using the same equation of state, and the excess uptake of a slit pore is calculated by integrating the local excess density (subtracting the gas density where there is no adsorbent−adsorbate interaction) over the unit cell. The uptake N of an activated carbon is calculated using $N(P) = \sum_i \overline{\rho}_i(P) \times dV_i$, where $\overline{\rho}_i(P)$ and dV_i are the average density at pressure P and differential pore volume of the slit pore i, respectively. For both experiment and theory, the heat of adsorption was calculated from the isotherms of absolute uptake at 273 and 298 K, fitted to the Toth model[26] and using the Clausius−Clapeyron equation.

As the CH_4−graphene interaction shows little corrugation with an energy variation less than 4 meV (Figure S1, Supporting Information), the strongest binding site (with methane over the hexagonal ring center) was used to calculate the PES. The maximum binding of 166 meV between methane and a graphene sheet occurs at a separation distance of 3.5 Å. The CH_4−carbon slit pore interactions for various pore sizes are shown in Figure 1a. From these interactions, the local CH_4 density is calculated using our thermodynamic continuum approach; these density profiles are shown in Figure 1b for T = 298 K and P = 20 bar. Most regions in the 6 Å pore actually repel CH_4, except near the center of the pore. The 7 Å pore gives a narrow but deep potential well, with a maximum binding of 350 meV at its pore center, resulting in a maximum adsorption density of 34 mol/L at 298 K and 20 bar. This adsorption density is close to that of liquid methane at the triple point, suggesting that physisorption can provide strong adsorption in small carbon nanopores. The binding strength at the pore center decreases rapidly with increasing slit pore size for pores >7 Å, and a "double well" potential with two minima located away from the center of the pore starts to develop for a 9 Å slit pore (data not shown). As the pore size increases, the methane−graphene interaction is strongest near each of the single graphene layers, resulting in a lower methane density at the pore center. The excess gravimetric capacity reaches a maximum in 12 Å slit pores, with little changes for larger pores (Figure S2, Supporting Information).

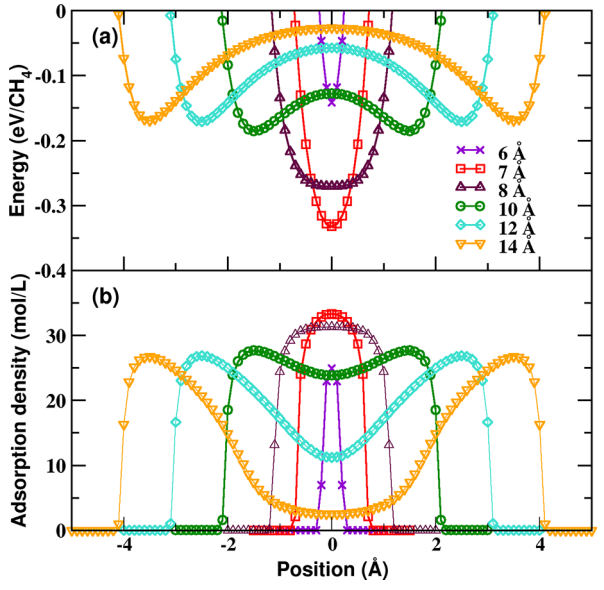

Figure 1. Pore size-dependent CH_4 adsorption of slit pores. (a) CH_4−slit pore interaction energy. (b) Adsorption density at T = 298 K and P = 20 bar.

In order to assess the capability of our approach for predicting gas storage capacity, the isotherms for five AC materials were measured at 298 K up to 20 bar (see Supporting Information for experimental details). The five ACs include lignin-derived carbon fiber physically activated in CO_2 at 52% burnoff (LACF), carbide-derived carbon (CDC), commercial AC Maxsorb, ultramicroporous carbon (UMC), and mesoporous AC (mesoAC) (see Supporting Information for details). The pore size distributions of these ACs, shown in Figure 2,

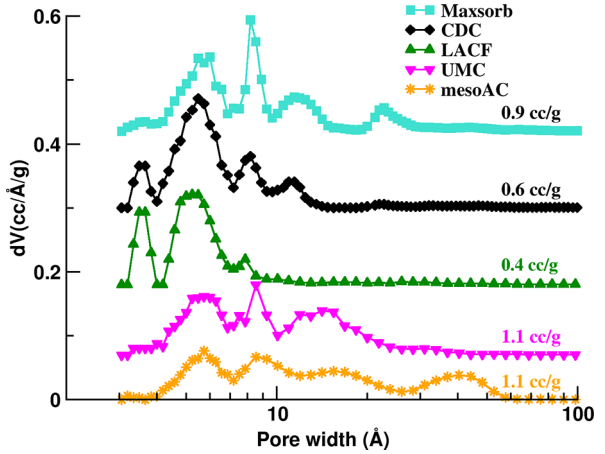

Figure 2. Pore size distribution of activated carbons. The numbers indicate the pore volume with the effective pore width ≤40 Å.

were determined using CO_2 and N_2 adsorption data analyzed using the nonlocal density functional theory (NLDFT)[7] for CO_2 data and the quenched surface model (QSDFT)[27] for N_2 data. It should be noted that whereas the pore size is defined by the distance between the carbon sheets in the slit pore model the experimental characterization uses an effective pore width, i.e., the interlayer distance with the carbon diameter of 3.4 Å excluded, similar to the description of Celzard et al.[28]

Figure 3 shows the comparison between the experimental and theoretical quantities at P = 20 bar. Theory correctly predicts that LACF and CDC are significantly poorer adsorbents than UMC, Maxsorb, and MesoAC, with UMC being the highest adsorbent. One could argue that this simply reflects the total pore volumes (Figure 2). Therefore, Figure 3b shows the excess adsorption normalized by the total pore volume (i.e., an average CH_4 density in the pores). There is a strong trend, accurately captured by the theory, showing that LACF and CDC have a much larger amount of CH_4 per unit pore volume. This is clearly reflected in the higher heats of adsorption of LACF and CDC, shown in Figure 3c. The approach correctly predicts that LACF has the highest heat of adsorption, and Maxsorb, UMC, and MesoAC have the lowest. The correlation between CH_4 density in the pores and heat of adsorption is related to their pore size distributions shown in

dx.doi.org/10.1021/ct400875n | J. Chem. Theory Comput. 2014, 10, 1−4

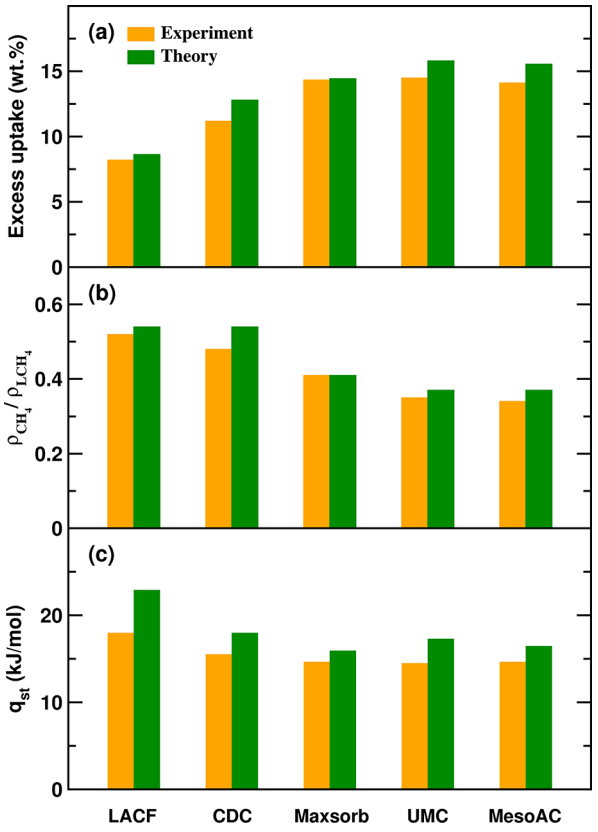

Figure 3. Comparison of the experiment and theory for (a) excess uptake at 298 K and 20 bar, (b) average methane density in pores compared to liquid methane density at triple point, and (c) isosteric heat of adsorption.

Figure 2. LACF is populated with relatively small pores with effective sizes less than 10 Å. From our experiments and calculations, we see that these small pores give strong binding of methane to AC but contribute little to the total pore volume, leading to high heat of adsorption but low uptake. This is consistent with our previous findings for H_2 in carbon materials; systems with small pores may have high heats of adsorption and high densities in the pores, while systems with large pores may have higher uptake but lower heats of adsorption.[29]

The remaining discrepancies between prediction and experiment shown in Figure 3 likely have contributions from three sources: experiments, calculated CH_4–graphene interactions, and thermodynamic model. The challenge in improving the comparison is that all three factors are intertwined, and it is difficult to test the effect of any single factor exclusively. On the experimental side, possible sources of errors come from temperature variations during measurements and from improper buoyancy corrections. In our experiments, the temperature was stabilized within ±0.05 °C using a circulating water bath. Buoyancy corrections were made using material density values estimated by helium displacement. Under these conditions, the accuracy of excess uptake measurements is estimated at ±0.01 wt % or better. We have also performed calculations of the interactions using the original vdW-DF[15] and vdW-DF2[30] functionals, and under the conditions shown in Figure 3, the adsorption trends are minimally affected. The vdW-DF^{C09x} functional produces the highest uptakes, while the vdW-DF2 consistently predicts approximately 20% less uptake (and approximately 15% less than experiment). Furthermore, our vdW-DF^{C09x} calculations are in good agreement with recent MP2 calculations for methane on coronene, albeit these are slightly more strongly bound than the CCSD(T) results.[31] If we assume a reasonable accuracy of vdW-DF^{C09x} and negligible uncertainty involved in the experiments, then the level of the agreement between the experiment and calculation would mainly be dictated by the thermodynamic model. The primary assumption of the thermodynamic model is that the methane adsorption mimics the pure gas behavior. This assumption is weakest when the methane is both dense and closely confined, i.e., when one should think of well-defined layers of adsorbed molecules. At high temperatures and low densities, however, and particularly when the corrugation of the substrate potential is weak, as is the present case, this should not be significant.

In summary, we have demonstrated a generalizable scheme for an efficient, electronic structure-based approach to predicting pore size-dependent adsorption, leading to total uptakes, without empirical potentials or lengthy simulations. We utilized the recently developed vdW-DF and incorporated these interactions into our thermodynamic continuum method to accurately predict the methane storage capacity of activated carbons. We theoretically predict and experimentally observe that methane strongly binds to narrow pores, leading to higher methane densities in the pores of sizes close to 7 Å. Above this value, the density of the adsorbed methane decreases with increasing pore size. However, the excess uptakes increase up to 12 Å pores due to the increased volume. Remarkably, we can rank these materials both in terms of excess uptake, density of adsorbate in the pores, and heats of adsorption, despite the simplicity of the slit pore model relative to the complexity of real pore structures.[7,19,21] Such results allow us to better understand the origin of the higher heats of adsorption in ACs with seemingly lower total uptake. Our method provides an inexpensive but reasonably accurate prediction for gas adsorption on micropores, which opens up a new avenue for rational design of materials for physisorption-based gas storage, capture, and separation using a high-throughput screening approach, including other types of nanoporous materials that could benefit from this model, such as molecular crystals, zeolites, and metal organic framework.

■ ASSOCIATED CONTENT

Ⓢ Supporting Information

Sample details, experimental details for the pore size distribution and gravimetric capacity measurements, van der Waals density functional method, prediction for pore size-dependent methane adsorption, and comparison between experiment and theory. This material is available free of charge via the Internet at http://pubs.acs.org.

■ AUTHOR INFORMATION

Corresponding Authors

*E-mail: coopervr@ornl.gov (V.R.C.).
*E-mail: morrisj@ornl.gov (J.R.M.).

Notes

The authors declare no competing financial interest.

■ ACKNOWLEDGMENTS

We thank Raina Olsen for critical reading of the manuscript. This work was supported by the Materials Sciences and Engineering Division, Office of Basic Energy Sciences, U.S.

Department of Energy. This research used resources of the National Energy Research Scientific Computing Center, supported by the Office of Science, U.S. Department of Energy under Contract No. DEAC02-05CH11231.

REFERENCES

(1) Panella, B.; Hirscher, M.; Roth, S. *Carbon* **2005**, *43*, 2209.
(2) Duren, T.; Bae, Y. S.; Snurr, R. Q. *Chem. Soc. Rev.* **2009**, *38*, 1237.
(3) Aga, R. S.; Fu, C. L.; Krcmar, M.; Morris, J. R. *Phys. Rev. B* **2007**, *76*, 165404.
(4) Gallego, N. C.; He, L. L.; Saha, D.; Contescu, C. I.; Melnichenko, Y. B. *J. Am. Chem. Soc.* **2011**, *133*, 13794.
(5) Steele, W. A. *Surf. Sci.* **1973**, *36*, 317.
(6) Garcia-Perez, E.; Parra, J. B.; Ania, C. O.; Garcia-Sanchez, A.; Van Baten, J. M.; Krishna, R.; Dubbeldam, D.; Calero, S. *Adsorption* **2007**, *13*, 469.
(7) Lastoskie, C.; Gubbins, K. E.; Quirke, N. *Langmuir* **1993**, *9*, 2693.
(8) Matranga, K. R.; Myers, A. L.; Glandt, E. D. *Chem. Eng. Sci.* **1992**, *47*, 1569.
(9) Jagiello, J.; Anson, A.; Martinez, M. T. *J. Phys. Chem. B* **2006**, *110*, 4531.
(10) Kim, J.; Maiti, A.; Lin, L. C.; Stolaroff, J. K.; Smit, B.; Aines, R. D. *Nat. Commun.* **2013**, *4*, 1694.
(11) Lin, L. C.; Berger, A. H.; Martin, R. L.; Kim, J.; Swisher, J. A.; Jariwala, K.; Rycroft, C. H.; Bhown, A. S.; Deem, M.; Haranczyk, M.; Smit, B. *Nat. Mater.* **2012**, *11*, 633.
(12) Wilmer, C. E.; Leaf, M.; Lee, C. Y.; Farha, O. K.; Hauser, B. G.; Hupp, J. T.; Snurr, R. Q. *Nat. Chem.* **2012**, *4*, 83.
(13) Sillar, K.; Sauer, J. *J. Am. Chem. Soc.* **2012**, *134*, 18354.
(14) Kong, X.; Deng, H.; Yan, F.; Kim, J.; Swisher, J. A.; Smit, B.; Yaghi, O. M.; Reimer, J. A. *Science* **2013**, *341*, 882.
(15) Dion, M.; Rydberg, H.; Schroder, E.; Langreth, D. C.; Lundqvist, B. I. *Phys. Rev. Lett.* **2004**, *92*, 246401.
(16) Cooper, V. R. *Phys. Rev. B* **2010**, *81*, 161104.
(17) Peng, L. J.; Morris, J. R. *J. Phys. Chem. C* **2010**, *114*, 15522.
(18) Ihm, Y.; Cooper, V. R.; Peng, L.; Morris, J. R. *J. Phys.: Condens. Matter* **2012**, *24*, 424205.
(19) Guo, J.; Morris, J. R.; Ihm, Y.; Contescu, C. I.; Gallego, N. C.; Duscher, G.; Pennycook, S. J.; Chisholm, M. F. *Small* **2012**, *8*, 3283.
(20) Dmowski, W.; Contescu, C. I.; Llobet, A.; Gallego, N. C.; Egami, T. *J. Phys. Chem. C* **2012**, *116*, 2946.
(21) Morris, J. R.; Contescu, C. I.; Chisholm, M. F.; Cooper, V. R.; Guo, J.; He, L.; Ihm, Y.; Mamontov, E.; Melnichenko, Y. B.; Olsen, R. J.; Pennycook, S. J.; Stone, M. B.; Zhang, H.; Gallego, N. C. *J. Mater. Chem. A* **2013**, *1*, 9341.
(22) Thonhauser, T.; Cooper, V. R.; Li, S.; Puzder, A.; Hyldgaard, P.; Langreth, D. C. *Phys. Rev. B* **2007**, *76*, 125112.
(23) Paolo, G.; Stefano, B.; Nicola, B.; Matteo, C.; Roberto, C.; Carlo, C.; Davide, C.; Guido, L. C.; Matteo, C.; Ismaila, D.; Andrea Dal, C.; Stefano de, G.; Stefano, F.; Guido, F.; Ralph, G.; Uwe, G.; Christos, G.; Anton, K.; Michele, L.; Layla, M.-S.; Nicola, M.; Francesco, M.; Riccardo, M.; Stefano, P.; Alfredo, P.; Lorenzo, P.; Carlo, S.; Sandro, S.; Gabriele, S.; Ari, P. S.; Alexander, S.; Paolo, U.; Renata, M. W. *J. Phys.: Condens. Matter* **2009**, *21*, 395502.
(24) Cooper, V. R.; Ihm, Y.; Morris, J. R. *Phys. Procedia* **2012**, *34*, 34.
(25) Setzmann, U.; Wagner, W. *J. Phys. Chem. Ref. Data* **1991**, *20*, 1061.
(26) Foo, K. Y.; Hameed, B. H. *Chem. Eng. J.* **2010**, *156*, 2.
(27) Ravikovitch, P. I.; Neimark, A. V. *Langmuir* **2006**, *22*, 11171.
(28) Celzard, A.; Fierro, V. *Energy Fuel* **2005**, *19*, 573.
(29) Peng, L. J.; Morris, J. R. *Carbon* **2012**, *50*, 1394.
(30) Lee, K.; Murray, E. D.; Kong, L.; Lundqvist, B. I.; Langreth, D. C. *Phys. Rev. B* **2010**, *82*, 081101.
(31) Smith, D. G. A.; Patkowski, K. *J. Chem. Theory Comput.* **2012**, *9*, 370.